



Radio Science

RESEARCH ARTICLE

10.1002/2015RS005695

Key Points:

- Annual rain fade distributions can be estimated from a small set of rain fields
- An optimized algorithm is presented and yields the best fit to annual distributions
- As few as 200 rain fields can be used to estimate annual distributions

Correspondence to:

K. S. Paulson,
k.paulson@hull.ac.uk

Citation:

Paulson, K. S., and I. D. Chinda (2015), Prediction of annual joint rain fade on EHF networks by weighted rain field selection, *Radio Sci.*, 50, doi:10.1002/2015RS005695.

Received 2 MAR 2015

Accepted 28 JUL 2015

Accepted article online 1 AUG 2015

Prediction of annual joint rain fade on EHF networks by weighted rain field selection

K. S. Paulson¹ and I. D. Chinda¹

¹School of Engineering, University of Hull, Hull, UK

Abstract We present a computationally efficient method to predict joint rain fade on arbitrary networks of microwave links. Methods based on synthetic rain fields composed of a superposition of rain cells have been shown to produce useful predictions of joint fade, with low computational overhead. Other methods using rain fields derived from radar systems have much higher computational overhead but provide better predictions. The proposed method combines the best features of both methods by using a small number of measured rain fields to produce annual fade predictions. Rain fields are grouped into heavy rain and light rain groups by maximum rain rate. A small selection of rain fields from each group are downscaled and fade predictions generated by pseudointegration of specific attenuation. This paper presents a method to optimize the weights used to combine the heavy rain and light rain fade predictions to yield an estimate of the average annual distribution. The algorithm presented yields estimates of average annual fade distributions with an error small compared to year-to-year variation, using only 0.2% of the annual data set of rain fields.

1. Introduction

The International Telecommunication Union-Radiocommunication Sector (ITU-R) maintains a set of internationally recognized propagation models. These provide predictions of average annual distributions of 1 min fade averages, on individual terrestrial and Earth-space radio links, for any point on Earth. These models are used for the regulation and coordination of radio systems by national spectrum regulators. They are also used for the estimation of link budgets on Earth-space and terrestrial links. The ITU-R also provides models specifically for the design of Fade Mitigation Techniques (FMTs). These include models of fade duration and fade slope for a 10 s integration time, and Rec. ITU-R P.1853-0 which provides a method for dynamic fade time series synthesis for individual links. However, the design and optimization of Dynamic Network Management (DNM) tools requires joint channel models applicable to arbitrarily complex, heterogeneous networks of links. Furthermore, as the definition of outage and Quality of Service depends upon second-to-second performance of a network, much higher temporal resolution is required.

The dominant dynamic fade mechanisms at EHF are scattering by liquid and solid hydrometeors and cloud droplets, multipath, and scintillation. These fade mechanisms exhibit complex spatial and temporal correlations, over a wide range of scales. Furthermore, for network simulation, it is necessary to be able to model the variation of these parameters over a very wide range of scales. The spatial scales range from a radio beam Fresnel diameter to the width of a network, while temporal scales range from 1 s fade variation to the lifetime of a large weather system. For DNM design and optimization it is necessary to be able to model the performance of a substantial part of a network and so these correlations need to be modeled.

A way to achieve this is to generate fine-scale, spatial-temporal fields of specific attenuation and then to simulate the fade on each radio link by pseudointegration along the link path. Hydrometeor-specific attenuation is related to rain rate by the power law of Rec. ITU-R P.838-3 and the sleet model of Rec. ITU-R P.530-15. Rain rate fields are known to vary rapidly in space and time. Other atmospheric fade mechanisms vary more slowly, for example, gaseous absorption. However, spatial-temporal rain rate fields are generally not available over the range of temporal and spatial scales required. Over some range of scales, the rain rate variation needs to be generated numerically. The final report of European Cooperation in Science and Technology Action IC0802, and a recent review paper [Paulson *et al.*, 2013], provided a taxonomy of simulation tools able to predict joint rain fade on arbitrary networks of EHF links. Classification was based on the method used to generate the rain fields. The three groups identified were rain cell methods, downscaled measured rain fields, and synthetic stochastic rain fields.

Two of the groups are relevant to the work reported in this paper: cell models and downscaling models. Rain cell methods generate fine-scale rain intensity fields by the aggregation of multiple, synthetic rain cells [Capsoni *et al.*, 2009]. Distributions of rain cell parameters, such as size, shape, maximum, and mean rain rate, have been studied since the 1980s [see Crane, 1980; Capsoni *et al.*, 1987]. The best known of the rain cell models is the EXCELL model [Capsoni *et al.*, 2009] and its recent enhancements: MultiEXCELL [Luini and Capsoni, 2011] and the HYCELL model [Féral *et al.*, 2003]. Several systems generate rain fields by the numerical-statistical downscaling of coarse rain fields, generally measured by radar or derived from Numerical Weather Prediction products. These include the University of Hull's Global Integrated Network Simulator (GINSIM) [Paulson and Basarudin, 2011]; the SATCOM system, developed by the University of Bath [Hodges *et al.*, 2006]; and the Simulator of the Space-Time behavior of the Attenuation due to Rain software developed at the French Aerospace Laboratory Office National d'Etudes et de Recherche Aéronautiques and the Centre National d'Études Spatiales [Carrie *et al.*, 2011].

These two groups of simulators differ radically in two major characteristics. The downscaling methods are capable of simulating time series of joint fade, while rain cell models aim to produce long-term joint fade statistics. The downscaling methods can also derive joint fade distributions from the generated time series. The extra functionality of time series is important when optimizing FMTs. Second, the rain cell models require a tiny fraction of the computational effort required by the methods dependent upon spatial-temporal downscaling. Downscaling can be subdivided into disaggregation and interpolation. Interpolation is usually considerably more computationally expensive than disaggregation.

A rain cell model will typically generate 500 to 1000 synthetic rain maps spanning regions approximately 200 km across. These maps have no time reference and can be thought of as independent samples from the distribution of rain fields possible in an average year. The maps are used to produce single or joint fade estimates and the whole process requires only a few seconds of computation on a PC. By contrast, GINSIM requires at least a year of measured rain field data. For the UK Meteorological Office Nimrod composite rain images, this corresponds to 105,120 fields with a 5 min sample time [Chinda and Paulson, 2014]. Spatial disaggregation from 1 km to 125 m resolution is relatively fast but increases the amount of data in each rain field by a factor of 64. GINSIM then interpolates these to 18.75 s sample time, yielding 3.4 million fields. For a 200 km square region, this results in 4×10^{12} samples requiring 10 Tb of storage. These need only be calculated once for a climate of interest, but it is likely that several years of data will be required for most applications. From these data, GINSIM can predict joint fade time series for arbitrary networks, for specific periods of time, with unsurpassed accuracy. However, the complexity and computational intensity of GINSIM has greatly constrained its use. The principal reason for the superior performance is that the measured rain fields reproduce the spatial complexity present in rain far better than the pulse models with their simple cell profiles, [Paulson *et al.*, 2014].

This paper investigates a simulation method using the best features of both systems, i.e., the use of a carefully chosen subset of measured rain fields. The use of coarse-scaled measured rain fields removes the greatest source of error from the rain cell methods, i.e., poorly approximated spatial rain rate covariance. Measured fields include complex features such as clusters of convective cells within fronts and orographic effects caused by landscape features. A small number of measured fields are chosen, typically a few hundreds, to match the long-term rain rate distribution. These fields are downscaled and then transformed into specific attenuation fields and used to estimate joint fade distributions in the usual way. The GINSIM-WeightedSelect method developed in this paper is an extension to the GINSIM-Select method presented in EUCAP14 [Chinda and Paulson, 2014]. Unlike the earlier method, WeightedSelect does not require a priori knowledge of the annual proportions of classes of rain field and also yields superior results. Furthermore, we present tests against measured, joint link data.

This paper is organized as follows. Section 2 summarizes the stochastic downscaling of rain fields. Sections 3 and 4 introduce and define the GINSIM-WeightedSelect algorithm. Section 5 investigates the performance of the proposed method in predicting distributions of fade on a range of terrestrial and Earth-space links. Predictions are compared to measured data on a terrestrial link and several Earth-space links, available from Callaghan *et al.* [2011] and described in Callaghan *et al.* [2013]. Section 6 draws conclusions.

2. Downscaling Data

The UK Meteorological Office operates the Nimrod network of 15 C band rain radars operating at 5.4 GHz [UK Meteorological Office, 2003]. For this analysis we use composite measured maps of instantaneous rain

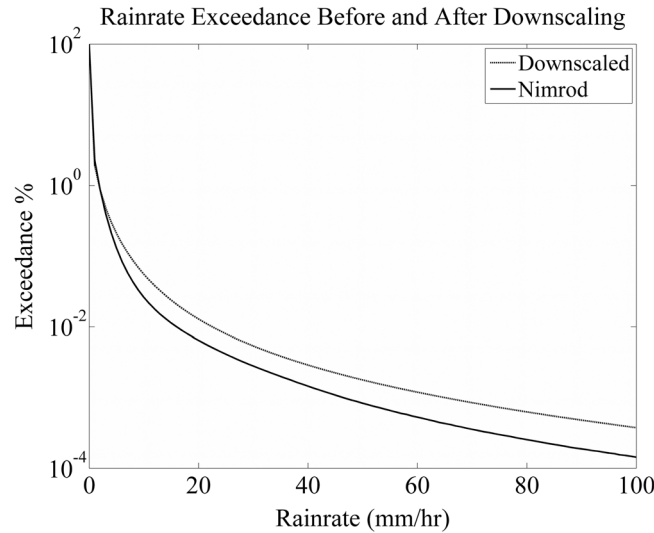


Figure 1. Rain rate exceedance distribution analysis for 1 km Nimrod data and downsampled 125 m data.

rate over approximately 1 km squares, spanning a 200 km region in the south of UK, with a 5 min sample period. The data used in this project span from 2004 to 2006 and are currently archived with the British Atmospheric Data Centre.

Rain rates derived from smaller integration volumes exhibit more extremes and faster variation. If fade is needed on links shorter than a few kilometers, or over intervals of time shorter than 1 min, then rain rate data are required at higher resolution than those provided by Nimrod. This can be achieved by numerical downscaling, i.e., using a stochastic numerical algorithm to introduce the fine-scale variation not present in the coarse-scale data.

Data from Nimrod are approximately rain rate averages over 1 km squares. Disaggregation is the process of producing possible fine-scale rain fields constrained by the coarse-scale aggregates provided by Nimrod. In GINSIM, disaggregation is achieved using the multiplicative cascade algorithm of Deidda [Deidda, 2000] and [Paulson and Zhang, 2009]. The Deidda method replaces each rain rate R_{Δ} averaged over a 2-D region of diameter Δ , with four rain rates $R_{\Delta/2}^i = w_i R_{\Delta}$, $i = 1, 2, 3, 4$, averaged over regions of diameter $\Delta/2$. The weights w_i are independent and identically distributed samples from a log-Poisson distribution: $w_i = e^{a\beta y}$, where y is an independent and identically distributed sample from a Poisson distribution of mean c . The parameters β and c are determined by fitting the scaling exponents of the cascade to measured values. The normalizing constant $a = c(1 - \beta)$ is determined by the canonical first-order constraint; i.e., $E(w_i) = 1$. Using the multifractal exponents reported in Paulson and Zhang [2007] yields the parameters $c = 10$ and $\beta = 1.115$ for region diameters below 2 km. The multiplicative cascade disaggregation algorithm is computationally efficient, and the numerical effort associated with downscaling is insignificant compared to that required for interpolation in GINSIM [Paulson and Basarudin, 2011; Basarudin, 2012].

Figure 1 illustrates the rain rate exceedance distribution calculated from 3 years of Nimrod composite rain data over a square of width 200 km centered on Chilbolton in the southern UK. Also shown is the distribution of rain rates after downscaling by a factor of 8 to squares of width 125 m. As expected, downscaling increases the proportion of extreme rain rates and, in this case, increases the rain rate exceeded for 0.01% of time from approximately 20 mm/h to 30 mm/h. Basarudin [2012] has shown that downscaling over this range improves estimation of link fade distributions. Further downscaling increases computational effort and data storage

requirements but yields little improvement in fade estimation for links longer than a few kilometers.

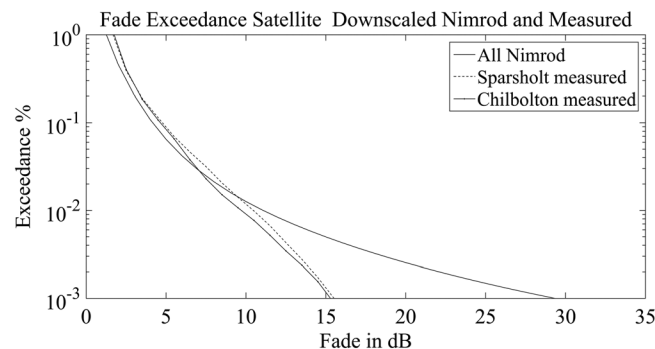


Figure 2. Fade exceedance distributions for Ka band Earth-space links and simulated links using downsampled Nimrod data.

Figure 2 shows a comparison between the fade exceedance measured on two Earth-space links, operated by Rutherford Appleton Laboratory, and a prediction based on downsampled Nimrod rain fields. The links operated between a 20.7 GHz beacon on a Global Broadcast System satellite and ground stations separated by 9 km at Chilbolton and Sparsholt in the southern UK. The receivers had a measurement

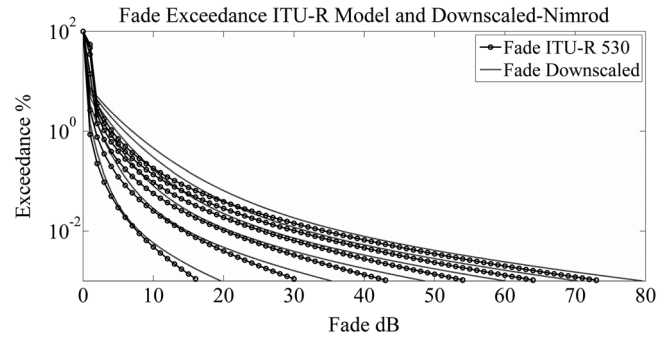


Figure 3. Fade exceedance distribution for six 38 GHz links of lengths 2, 4, 6, 8, 10, and 12 km; compared with the predictions of Rec. ITU-R 530-15 model.

dynamic range of approximately 13 dB. Dynamic fade intensity is the difference between the receive power and a notional clear-sky level. This level exhibited some oscillation due to orbit eccentricity. After removal of variation with a 24 h period, some drift in the clear-sky level remained. This limits the large fades that can be accurately measured to around 13 dB. Larger fades are recorded but are not reliable. Approximately 2 years of data are available, from August 2003 to March 2005. Fade predictions were also calculated using downscaled Nimrod data from

the same period. The rain height was assumed to have an average annual value provided by Rec. ITU-R P.839-4 and an annual distribution used in the sleet model of Rec. ITU-R P.530-15. Over the dynamic range of the measurements, the simulated and measured data are within measurement accuracy. Only rain fade has been simulated, and so some underestimation is expected due to other fade mechanisms, e.g., multipath. Rain fade is the dominant fade mechanism leading to outage, at frequencies above 5 GHz, and so simulated fades should be a good estimate of measured fades at time percentages below approximately 1%.

Figure 3 compares simulated fade distributions with ITU-R model predictions. Six, notional, 38 GHz, vertically polarized, terrestrial links, of lengths 2, 4, 6, 8, 10, and 12 km were simulated using 3 years of downscaled Nimrod data. These are compared with the predictions of Rec. ITU-R P.530-15, using a 0.01% exceeded rain rate of 30 mm/h. Around the important time percentage of 0.01%, the simulated and model results agree well. At higher time percentages, 0.1% to 1%, agreement is poor for longer links indicating that the ITU-R model underestimates the effects of light rain. Some variation from the average annual distribution is expected in the 3 year data set.

3. GINSIM-WeightedSelect: Introduction

In this paper, we propose a new method known as GINSIM-WeightedSelect. This method uses only a small selection of measured rain fields over the period of interest to estimate the long-term distributions of rain fade. Average annual results are estimated using a weighted sum of the fade distributions produced from classes of rain fields with different maximum rain rates.

As only a small number of rain maps are analyzed, the computational effort is quite small, similar to that required by MultiEXCELL. However, as measured rain fields are used, the predictions are more accurate than those from cell methods. The very large reduction in computational effort, compared to GINSIM, comes from the following: (1) no temporal interpolation is required as time series are not produced, (2) relatively small numbers of Nimrod rain maps containing rain are required, and (3) optimizing the weighted average of distributions yields better estimates using less data.

Terrestrial fixed links are engineered for availabilities of 99.99% or 99.999% in an average year. This corresponds to total annual outages of approximately 50 min and 5 min, respectively. Earth-space and mobile systems are often engineered to similar availabilities. As a consequence, the 105,120 Nimrod rain fields collected over a year will contain only 10 or so where a rain event associated with outage will affect a particular link. The number of scans containing rain events associated with outage on any link in a region 200 km across is over 1000. This increase is principally due to convective events, 5 to 10 km in diameter, with lifetimes of tens of minutes, which affect only small subregions. Many rain fields 200 km across will contain such events without them affecting a particular link. As the region area grows, the proportion that contains a rain event that would cause outage on a link somewhere in the region also grows.

Over a region with a homogenous climate, temporal averaging can be partially replaced by spatial averaging. A network can be placed anywhere in the rain fields, and at any rotation, and provide a valid joint fade sample. This implies that valid long-term statistics of joint fade could be estimated from a relatively small

number of rain fields, certainly less than 105,120. The GINSIM-WeightedSelect system aims to produce a substantial decrease in the number of Nimrod rain maps required, and the associated computational effort, by using a weighted sum of the fades produced by a small selection of rain fields.

4. GINSIM-WeightedSelect: Definition

The method assumes that the user has access to rain field data over a homogeneous climate area. This paper used Nimrod composite rain rate images over a square of width 200 km. Rain fields are classified into no rain, light rain, and heavy rain based on the highest rain rate present. Fields containing a rain rate above the 0.01% exceeded rain rate, at the measured scale, are classified as “heavy rain.” Fields with no rain are classified as “no rain,” and the rest are classified as “light rain.”

First, the user selects a small number of rain fields from each of the light rain and heavy rain categories. Data could be chosen based on historical knowledge of weather reports or network performance. Selected rain fields are downscaled and rain rate complementary cumulative probability functions (CCPF or exceedance) are calculated for each class: $X_0 \equiv \hat{\partial}(R)$, X_{Light} , and X_{Heavy} , where $\hat{\partial}(R)$ is the Dirac delta function and R is the rain rate.

An estimate of the long-term rain rate CCPF can be formed from a weighted sum of these three exceedances:

$$X(R) = W_0 X_0(R) + W_{Light} X_{Light}(R) + W_{Heavy} X_{Heavy}(R) \quad (1)$$

GINSIM-WeightedSelect uses post a priori weights calculated by optimizing the fit of the rain rate CCPF to a target distribution: $X_T(R)$. This could be obtained from Rec. ITU-R P.837 or from local rain gauge records. Define the matrices

$$\mathbf{X} \equiv (\mathbf{X}_0 \quad \mathbf{X}_{Light} \quad \mathbf{X}_{Heavy}) \quad (2a)$$

$$\mathbf{W} \equiv (W_0 \quad W_{Light} \quad W_{Heavy})^t \quad (2b)$$

where the vector quantities are discrete CCPF evaluated at specific rain rates. The weights can be calculated using the Moore-Penrose solution to the weighted least squares (LSQ) problem, i.e.,

$$\min_{\mathbf{W}} |\mathbf{K}(\mathbf{X}\mathbf{W} - \mathbf{X}_T)|^2 \quad (3)$$

The diagonal matrix \mathbf{K} provides the LSQ weights and has been chosen to be

$$\mathbf{K}_{ii} = \begin{cases} X_T^{-1}(R_i) & X_T(R_i) > 10^{-5} \\ 0 & \text{else} \end{cases} \quad (4)$$

This choice means that the LSQ solution approximately minimizes the sum of the squared relative errors, and approximates the Rec. ITU-R P.311-14 goodness of fit metric. It also removes sensitivity to rain rates with very low exceedance probabilities, which are highly variable and of less interest to radio engineers. The solution can be found by solving the symmetric, 3×3 , linear system:

$$\mathbf{X}'\mathbf{K}^2\mathbf{X}\mathbf{W} = \mathbf{X}'\mathbf{K}\mathbf{X}_T \quad (5)$$

A hypothesis to be tested is that the same weights can be used to produce an estimate of link hydrometeor fade distributions. Let $Y_L \equiv P(A > a)$ be the CCPF of hydrometeor fade, A , for the link L . Define class fade exceedance distributions Y_{Light} and Y_{Heavy} as the CCPF estimated from the same selection of downscaled rain fields belonging to the classes of light rain and heavy rain, respectively. Each downscaled rain field is transformed into a specific attenuation field using the power law of Rec. ITU-R P.838-3, and then a large number of link rain fade estimates are formed by pseudointegration of the specific attenuation along paths of the required length. For Earth-space links the pseudointegration is along the slant path and specific attenuation is assumed to vary with height following the Rec. ITU-R P.530-15 sleet enhancement factor. All the fades from the rain maps of each class are used to estimate the class CCPF. For the no rain fields $Y_0 \equiv \hat{\partial}(A)$. We will test the hypothesis that

$$Y_L(A) = W_0 Y_0(A) + W_{Light} Y_{Light}(A) + W_{Heavy} Y_{Heavy}(A) \quad (6)$$

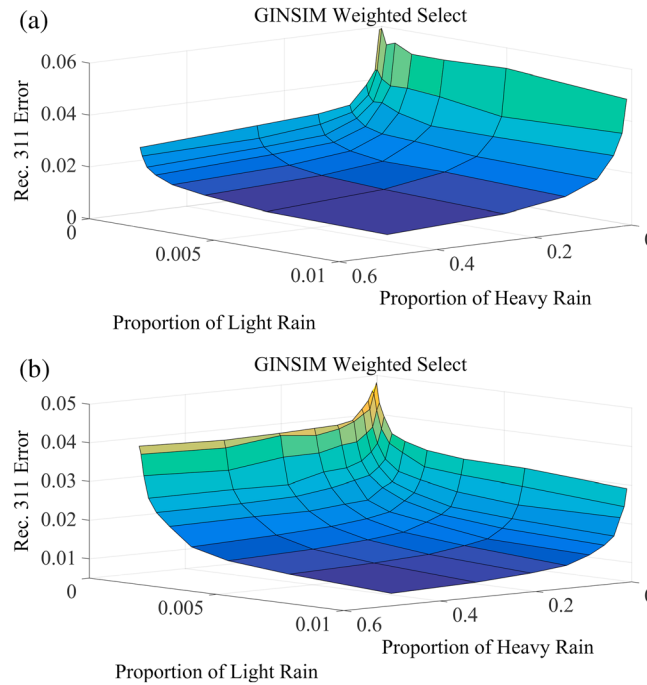


Figure 4. Error when estimating a specific year distribution of (a) rain rate and (b) rain fade on a notional 12 km, 38 GHz terrestrial link.

the ability to predict long-term rain and rain fade distributions. The average annual distribution is approximated using all the 3 years of Nimrod data. Distributions derived from different sized, random, selections of fields are tested to see how close they match the long-term distribution. In all tests, the error measure, ρ , is that defined in Rec. ITU-R P.311-14 and is calculated from the rain or rain fade exceeded at the time percentages: 0.001%, 0.002%, 0.003%, 0.005%, 0.01%, 0.02%, 0.03%, 0.05%, and 0.1%. Finally, the WeightedSelect method is used to predict the fade distribution on the 20.7 GHz Earth-space link data presented earlier and the joint distribution of fades on the convergent terrestrial and Earth-space links.

Figure 4a illustrates the error when using a selection of rain fields to estimate annual rain rate exceedance, compared to all downscaled Nimrod rain fields for a specific 1 year period. The typical error between a single year and the 3 year average is $\rho \approx 0.09$, and between 1 year and the Rec. ITU-R P.530-15 prediction, using the same 0.01% exceeded rain rate, is $\rho \approx 0.08$. These are measures of year-to-year variation around average annual results. It can be seen that the errors introduced by using a small selection of scans is small relative to the error due to year-to-year variability. Figure 4b shows the associated error when rain fade is estimated for a 12 km, 38 GHz terrestrial link using the same selection of fields as in Figure 4a. These figures show that fade errors smaller than those due to year-to-year variation can be achieved using a very small selection of rain field data, i.e., 0.2% of light rain fields and 10% of heavy rain fields. This corresponds to approximately 100 light and 100 heavy fields, i.e., a total of 200 rain fields or only slightly more than 0.2% of the total. Therefore, GINSIM-WeightedSelect requires only 1/500 of the computational effort of GINSIM to produce estimates of rain or rain fade distributions for a specific year, with an uncertainty less than that due to year-to-year variability.

A similar numerical experiment can be performed to see how well the long-term distribution can be estimated. Rec. ITU-R P.311-14 states that average annual distributions require a minimum of 3 years of data, and so we take the average distributions of rain rate and rain fade from the 3 years of downscaled Nimrod data as an estimate of the average annual distribution. Small random selections of light and heavy rain fields from the 3 year period are used to estimate these distributions. This test is very similar to the previous test, but now the distribution calculated from 3 years of data is estimated from samples of light and heavy rain fields from across the 3 years. Figure 5 presents the errors as functions of sample sizes. The results are very similar to the results for a specific year, and the conclusions are the same.

Equivalently, using the discretized distributions,

$$\mathbf{Y} \equiv (\mathbf{Y}_0 \quad \mathbf{Y}_{\text{Light}} \quad \mathbf{Y}_{\text{Heavy}}) \quad (7a)$$

$$\mathbf{Y}_L = \mathbf{Y}\mathbf{W} \quad (7b)$$

5. GINSIM-WeightedSelect Testing

The method specified in section 4 will be tested using the 3 year data set of Nimrod composite rain fields. Predictions will be compared with the 2 years of measured Earth-space link fade data presented in Figure 2 and simultaneous data from a 38 GHz, 5 km terrestrial link between South Wonston and the Sparsholt ground station.

Two tests are performed using a notional 12 km, 38 GHz terrestrial link. The first test uses specific years of data to test how well selections of fields from that year yield distributions that match the annual distribution. The second tests

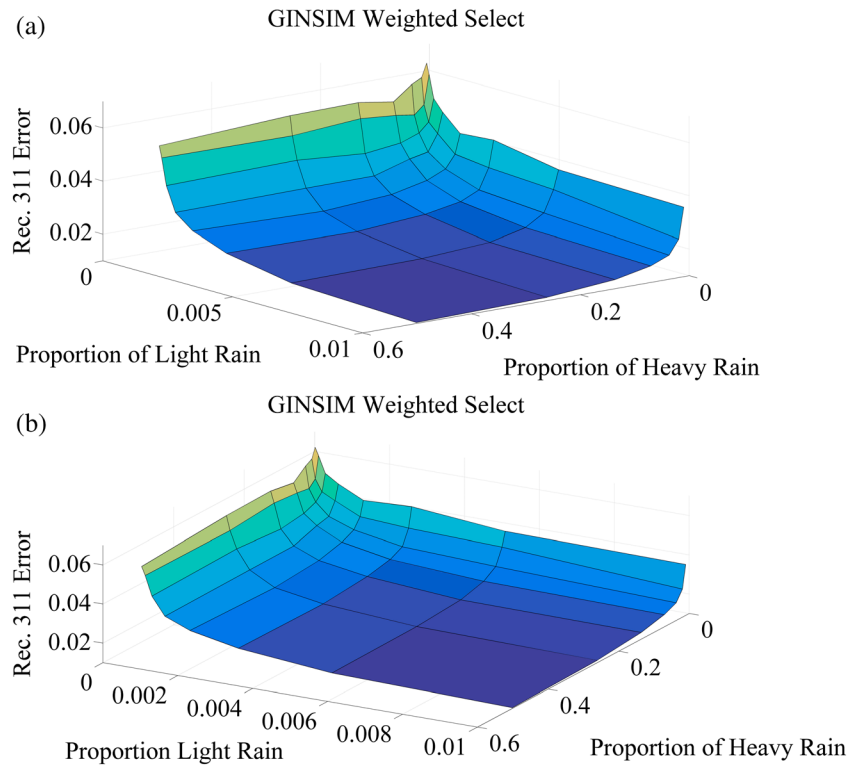


Figure 5. Error when estimating the average annual distribution of (a) rain rate and (b) rain fade on a notional 12 km, 38 GHz terrestrial link.

Finally, 2 years of data from the Earth-space link are considered. Simulation using all the downscaled Nimrod rain fields over the measurement period yields a good estimate of the fade distribution, up to the dynamic range of the measurement equipment, see Figure 2. Above approximately 12 dB, the simulation result is more plausible than the measured results. Given this, numerical tests will determine how well predictions based on small selections of rain fields approximate the result in Figure 2, derived from all Nimrod fields over the 2 years of measurements. Figure 6 presents these results. Once again, the errors are much smaller than those due to year-to-year variability.

Furthermore, they show considerable resilience to the number of light rain fields in the sample.

Earth-space links are more challenging to simulate due to the effects of variable rain height. We have assumed that rain height can be chosen independently from when the field was measured. Given this assumption, each selected rain field may be used to generate fade estimates using the same distribution of rain heights. In this case we use the Rec. ITU-R P.530-15 distribution around the Rec. ITU-R P.839-4 mean level. This appears to work well for the UK data. It will not work in regions where the rain type exhibits strong seasonality. For example, if small but intense convective storms only

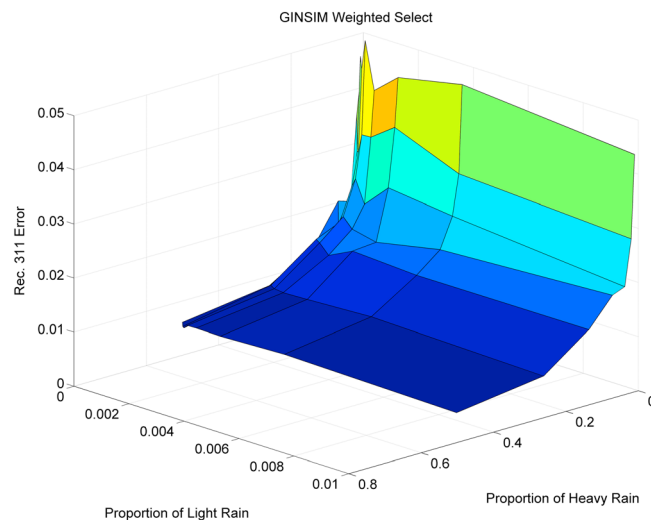


Figure 6. Error when estimating the annual distribution of rain fade on a 20.7 GHz Earth-space link.

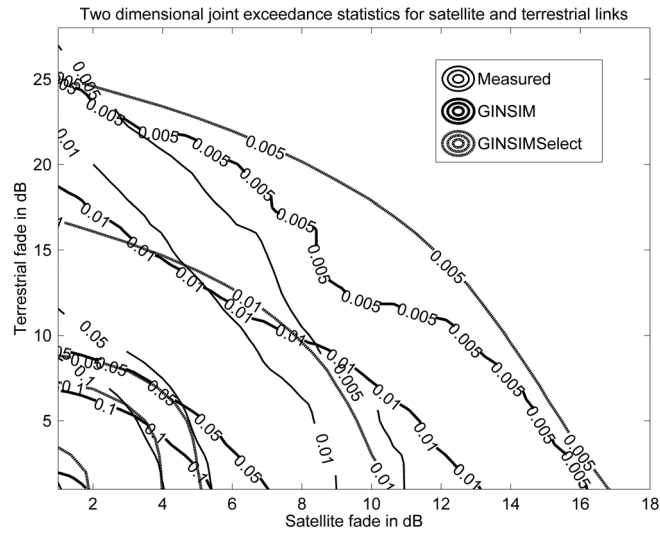


Figure 7. Two-dimensional joint fade exceedances using measured data and predictions using the GINSIM and WeightedSelect algorithms.

occur over summer, when the rain height is at its highest, then this technique would not work well. The distribution of rain heights appears to reduce the sensitivity to the variability between light rain fields.

Figure 7 illustrates the joint rain fade distribution for the convergent Earth-space link and a 5 km, 38 GHz terrestrial link. The differences between the two simulation methods, GINSIM and WeightedSelect, are due to the selection process, interpolated rain fields, and the way rain height is implemented. GINSIM uses the rain height at the time, derived from NOAA Reanalysis data, while WeightedSelect uses the annual distribution of rain heights. For these reasons, WeightedSelect

produces a smooth prediction closer to the average annual distribution, while GINSIM produces a result from a particular year constrained by the input rain fields. GINSIM is a stochastic simulator, and so multiple runs would produce different results that would converge to smoother result, but one still different from WeightedSelect if rain height and event intensity were correlated. The measured Earth-space fade distribution is constrained by the dynamic range of the measurement equipment for fades above 12 dB, and this leads to the increasing divergence between measured and predicted values, with decreasing exceedance probability, along the satellite fade axis.

6. Conclusions

We have developed an efficient method to estimate the rain fade exceedance distributions (CCPF) for arbitrary links. The method also yields joint distributions for arbitrarily complex networks of links. The method is based on the use of a small selection of rain fields derived from meteorological radar data, in this case the UK Nimrod radar network. It shares the large advantage of rain cell methods in requiring almost insignificant computational resource. It retains the advantage of measured rain field methods, such as GINSIM, of producing very accurate results, as rain fields with realistic autocovariance are used. It requires minimal amounts of a priori data. As few as 200 rain fields are adequate to produce annual exceedance distributions for a particular year: 100 light rain fields and 100 heavy rain fields. These data may be selected by the acquisition of data from rainy days based on weather reports or historical rain gauge records.

The computational effort required by the methods described in this paper can be decomposed into two parts. First, a collection of rain fields is required. MultiEXCELL produces around 500 rain fields using purely numerical methods conditioned by a known rain rate distribution. This requires less than a minute on a typical PC. GINSIM-WeightedSelect requires 100 light and 100 heavy rain fields. These could be selected by an automatic method, if many rain fields were already available, or rain fields from specific times could be acquired based on historical weather forecasts. Depending on the availability of these data, this stage may require direct human effort. Furthermore, the rain fields may require disaggregation. If all links are much longer than the spatial resolution of the field then disaggregation makes little difference to the predicted fade. To disaggregate a 200 km square rain field from 1 km resolution to 125 m resolution requires approximately 0.25 s on a standard office PC. Second, the methods use the rain fields to produce estimates of (joint) fade distributions. This effort is proportional to the number of rain fields, and so for 1 km resolution fields the Select methods are 60% faster than MultiEXCELL as they use 60% fewer fields. For disaggregated fields the computational effort is similar. Due to the spatial averaging, this stage requires approximately 1 s per rain field for a two-link network. As the same collection of rain fields may be reused any number of times for

arbitrary link networks, the computation effort of the second stage is the most important when evaluating the efficiency of the methods. When distributions are required, rather than time series, the Select methods are considerably less than 1/500 of the effort required by GINSIM as no temporal interpolation is required.

The tests reported in this paper assume the statistical independence of rain height and rain field characteristics, such as rain rate distribution and autocorrelation. This allowed an annual distribution of rain heights to be used with each rain field. However, the assumption will not be valid in regions where rain type (stratiform, convective, etc.) varies strongly with season, or where rain is concentrated in a cool or hot period of the year. This problem could be addressed to some extent by the use of annual distributions of rain height while raining. Rec. ITU-R P.839-4 also faces this criticism as it aims to present information on rain height during periods of precipitation but uses average annual 0° isotherm heights.

Simulators based on measured rain fields have been shown in other publications to yield better fade predictions than those based on synthetic rain fields. This has been attributed to the use of isotropic average annual rain rate autocorrelations when generating synthetic fields. Individual rain fields can be strongly anisotropic, e.g., fronts and squalls, and rain field types are expected to have different autocorrelations, e.g., convective events are expected to have relatively short correlation distances. Synthetic rain field methods would benefit from the integration of information on the structural variability of rain fields.

The method produces fade exceedance distributions but does not produce time series. However, it is also likely that the selection idea could be applied to rain events rather than rain fields. Each selected event would produce a time series using GINSIM downscaling techniques, from which temporal statistics such as joint fade slope and fade duration could be calculated. This is a new area to explore which is likely to yield a method to predict these statistics, with a similar decrease in computational effort compared to the existing GINSIM method.

Acknowledgments

The fade data for the terrestrial and satellite links and the UK Meteorological Office Nimrod data are available from the British Atmospheric Data Centre: badc.nerc.ac.uk.

References

- Basarudin H. (2012), Development of a heterogeneous microwave network, fade simulation tool applicable to networks that span Europe, PhD thesis, Univ. of Hull. [Available at hydra.hull.ac.uk/assets/hull:5774a/content.]
- Callaghan, S. A., J. Waight, C. J. Walden, J. Agnew, and S. Ventouras (2011), GBS 20.7 GHz slant path radio propagation measurements, Sparsholt site, [Internet]. British Atmospheric Data Centre, 2003–2005, 1 April, doi:10.5285/639a3714-bc74-46a6-9026-64931f355e07.
- Callaghan, S. A., J. Waight, J. Agnew, C. J. Walden, C. L. Wrench and S. Ventouras, (2013), The GBS dataset: Measurements of satellite site diversity at 20.7 GHz in the UK, *Geoscience Data Journal*, 17 March, doi:10.1002/gdj3.2.
- Capsoni, C., F. Fedi, C. Magistroni, A. Paraboni, and A. Pawlina (1987), Data and theory for a new model of the horizontal structure of rain cells for propagation applications, *Radio Sci.*, 22(3), 395–404, doi:10.1029/RS022i003p00395.
- Capsoni, C., L. Luini, A. Paraboni, C. Riva, and A. Martellucci (2009), A new prediction model of rain attenuation that separately accounts for stratiform and convective rain, *IEEE Trans. Antennas Propag.*, 57(1), 196–204.
- Carrie G., F. Lacoste, and Castanet L. (2011), New “on-demand” channel model to synthesize rain attenuation time series at Ku-, Ka- and Q/V-bands, *International Journal of Satellite Communications and Networking*, 29, 1, January/February, pp. 47–60.
- Chinda I. D., and K. S. Paulson, (2014), A computationally efficient system to predict joint rain fade on arbitrary EHF networks, The 8th European Conference on Antennas and Propagation (EuCAP 2014), Den Hague, pp. 3344–3348, 6–11 April.
- Crane, R. K. (1980), Prediction of attenuation by rain, *IEEE Trans. Commun.*, 28, 1717–1733.
- Deidda, R. (2000), Rainfall downscaling in a space-time multifractal framework, *Water Resour. Res.*, 36(7), 1779–1794, doi:10.1029/2000WR900038.
- Féral, L., H. Sauvageot, L. Castanet, and J. Lemorton (2003), HYCELL—A new hybrid model of the rain horizontal distribution for propagation studies: 1. Modeling of the rain cell, *Radio Sci.*, 38(3), 1056, doi:10.1029/2002RS002802.
- Hodges, D. D., R. J. Watson, and G. Wyman (2006), An attenuation time series model for propagation forecasting, *IEEE Trans. Antennas Propag.*, 54(6), 1726–1733.
- International Telecommunication Union (2005), Specific attenuation model for rain for use in prediction methods, ITU-R Recomm. P. 838-3, Geneva, Switzerland.
- International Telecommunication Union (2010), Tropospheric attenuation time series synthesis, ITU-R Recomm. P. 1853-0, Geneva, Switzerland.
- International Telecommunication Union (2012), Characteristics of precipitation for propagation modelling, ITU-R Recomm. P. 837-6, Geneva, Switzerland.
- International Telecommunication Union (2013a), Acquisition, presentation and analysis of data in studies of tropospheric propagation, ITU-R Recomm. P. 311-14, Geneva, Switzerland.
- International Telecommunication Union (2013b), Propagation data and prediction methods required for the design of terrestrial line-of-sight systems, ITU-R Recomm. P. 530-15, Geneva, Switzerland.
- International Telecommunication Union (2013c), Propagation data and prediction methods required for the design of Earth-space telecommunication systems, ITU-R Recomm. P. 618-11, Geneva, Switzerland.
- International Telecommunication Union (2013d), Rain height model for prediction methods, ITU-R Recomm. P. 839-4, Geneva, Switzerland.
- Luini, L. and C. Capsoni (2011), MultiEXCELL: A new rain field model for propagation applications, *IEEE Trans. Antennas Propag.*, 59(11), 4286–4300.
- Paulson K. S., and H. Basarudin (2011), Development of a heterogeneous microwave network fade simulation tool applicable to networks that span Europe, *Radio Sci.*, 46, RS4004, doi:10.1029/2010RS004608.
- Paulson, K. S., and X. B. Zhang (2007), Estimating the scaling of rain rate moments from radar and rain gauge, *J. Geophys. Res.*, 112, D20107, doi:10.1029/2007JD008547.

- Paulson, K. S. and X. B. Zhang, (2009), Simulation of rain fade on arbitrary microwave link networks by the downscaling and interpolation of rain radar data, *Radio Sci.*, 44, RS2013, doi:10.1029/2008RS003935.
- Paulson, K. S., L. Luini, N. Jeannin, B. Gremont, and R. Watson (2013), A review of channel simulators for heterogeneous microwave networks, *IEEE Antenn. Propag. Mag.*, 55(5), 118–127.
- Paulson, K. S., L. Luini, I. D. Chinda, and H. Basarudin (2014), Comparison of heterogeneous network rain fade simulation tools: GINSIM and MultiEXCELL, *IET Microwaves Antenn. Propag.*, doi:10.1049/iet-map.2014.0353.
- UK Meteorological Office (2003), Rain radar products (NIMROD) [Internet]. NCAS British Atmospheric Data Centre, 2003. [Available at http://badc.nerc.ac.uk/view/badc.nerc.ac.uk__ATOM__dataent_nimrod.]